Effect of κ-carrageenan film enriched with limonene extract and curcumin as an indicator of freshness

Hamdan, S. N. N.[1]**, Rovina, K.**[1*]**, Suriati, L.**[3]**, Pindi, W.**[2]**, Mantihal, S.**[2]**, Aris, N.**[2]**, Roslan, J.**[2]** and Huda, N.**[4]

[1]Faculty of Sustainable Agriculture, Universiti Malaysia Sabah, Locked Bag No. 3, 90509 Sandakan, Sabah, Malaysia; [2]Food Security Research Lab, Faculty of Food Science and Nutrition, University Malaysia Sabah, Kota Kinabalu, Sabah, Malaysia; [3]Department of Food Science and Technology, Faculty of Agriculture, Warmadewa University, Denpasar, Bali, Indonesia; [4]Postgraduate School, Universitas Brawijaya, Malang 65145, East Java, Indonesia.

Abstract This research investigated the creation of κ-carrageenan films incorporating limonene raw extract and curcumin, aiming to serve as effective freshness indicators in food packaging. Fourier Transform Infrared Spectroscopy and Field Emission Scanning Electron Microscopy were employed for film analysis. FTIR spectra indicated the presence of characteristic functional groups including O–H, C–H, C=C, C–O, C–OH, sulphate esters, C=O stretching, and CO–O–SO$_3$ stretching vibrations. FESEM imaging demonstrated a homogeneous surface with a dense and compact structure. The films' functional efficacy was assessed using chicken meat as a model system. The addition of curcumin and limonene facilitated observable color alterations corresponding to meat freshness, confirming the film's utility as a freshness indicator. In addition to indicating spoilage, these natural additives conferred antioxidant and antibacterial properties. The study underscored the potential of biodegradable κ-carrageenan films fortified with natural bioactive compounds as sustainable packaging solutions. However, further research is recommended to optimize limonene and curcumin concentrations and to validate their performance across diverse food matrices, thereby ensuring their commercial viability.

Keywords: Biodegradable plastics, Natural biopolymers, Limonene, Curcumin, Freshness indicator

Introduction

The American Society for Testing and Materials (ASTM) defines biodegradable plastics as polymeric materials capable of breaking down through the action of naturally occurring microorganisms, including bacteria, fungi, and algae (Shaikh *et al*., 2021). A wide variety of natural biopolymers such as pectin, lipids, proteins, chitosan, and starch have been investigated for this purpose

---

* **Corresponding Author:** Rovina, K. **Email:** rovinaruby@ums.edu.my

(Subbuvel and Kavan, 2022). These materials are generally considered non-toxic, inexpensive, sensitive, predictable, fast-acting, non-destructive, and non-invasive, making them attractive candidates for sustainable packaging applications. Consequently, recent research has emphasized the incorporation of pigments derived from plant sources and food waste into such biopolymers. Depending on their functionality, these polymers can be employed either individually or in combination. For instance, chitosan-based films have been explored as pH-sensitive indicators capable of visually detecting spoilage in beef and fish products. This approach addresses one of the major challenges in the packaging industry—monitoring the microbial spoilage of perishable foods (Liu *et al*., 2022).

Among perishable food products, chicken meat represents a highly consumed protein source that supplies essential amino acids to humans. However, it is prone to oxidative degradation, which reduces its quality. Lipid oxidation generates harmful compounds, including hypoxanthine (HX), xanthine, and ammonia, which compromise consumer safety (Abedi-Firoozjah *et al.,* 2023). HX, in particular, is a key purine metabolism product present in biological fluids, cells, and tissues, and is widely used as a biochemical marker. It provides insights into cell ageing, helps diagnose gout, cardiac, and cancer-related conditions, and serves as an indicator of meat freshness and spoilage (Varadaiah *et al.,* 2022). In response, many studies have developed biodegradable films incorporating curcumin as a bioactive component to monitor the freshness of chicken meat (Yildiz, 2022).

κ-carrageenan, a linear sulphated polysaccharide extracted from the red seaweed *Kappaphycus alvarezii*, has gained attention due to its strong gelling, emulsifying, and stabilizing capabilities. Its film-forming potential has led to applications in dairy, confectionery, and meat products. Owing to the presence of potassium ions (K$^+$), κ-carrageenan typically produces rigid, brittle gels. Compared with iota- and lambda-carrageenan, as well as polyethylene-based films, κ-carrageenan generates transparent films with superior tensile strength. Nonetheless, enhancements in mechanical properties and water vapor barrier performance are required for broader packaging applications (Liu *et al.,* 2020).

Limonene, a bioactive compound primarily extracted from citrus peels, possesses antioxidant, anti-inflammatory, and anticancer properties. Once isolated, it appears as a white powder and is widely used in consumer products such as perfumes, beverages, soaps, and detergents. Limonene also exhibits antibacterial activity by penetrating lipid membranes, disrupting cellular structures, and causing protein denaturation. Its demonstrated ability to inhibit the growth of bacteria, yeast, and fungi has been harnessed to extend the shelf

life of fresh produce, including strawberries, blueberries, and cucumbers (Shaw *et al*., 2023).

Curcumin, the principal bioactive compound in turmeric (*Curcuma longa L.*), is well known for its potent antioxidant activity. Rich in phenolic compounds, this natural polyphenol exhibits broad pharmacological effects, including anti-inflammatory, anticancer, and antimicrobial properties. Curcumin is also highly pH-sensitive: its phenolic hydroxyl groups undergo ionization under alkaline conditions to form phenoxide anions, leading to changes in color. This property not only enables curcumin to act as a pH-responsive indicator but also contributes to the scavenging of oxygen free radicals such as superoxide anions and hydroxyl radicals, which initiate lipid peroxidation (Rachtanapun *et al*., 2021). Therefore, the objective was to characterize the physicochemical properties of κ-carrageenan films enriched with curcumin and crude limonene extract and to elucidate their structure–property relationships.

Materials and methods

Raw material

Fresh orange fruit (*Citrus reticulata*), turmeric powder, and raw chicken meat were procured from a local supermarket in Kota Kinabalu, Sabah, Malaysia. Analytical grade chemicals, including ethanol, acetone, acetic acid, sodium hydroxide pellets, 2,2-diphenyl-1-picrylhydrazyl (DPPH), and κ-carrageenan powder, were sourced from Systerm Company (Malaysia), Merck (Germany), Merck (Germany), Sigma-Aldrich (United States), and Foodmate Co., Ltd. (Shanghai, China), respectively.

Extraction of crude extract of limonene from orange peel

Limonene extraction was carried out following the procedure described by Hasibuan and Gultom (2021), with slight modifications. Initially, pristine orange peels underwent a thorough cleaning process to eliminate any contaminants, followed by sun-drying and subsequent pulverization into a fine powder utilizing a blender. Orange peels were cleaned, dried in the sun, and ground into a fine powder. Subsequently, 25 g of this powder was combined with 350 mL of 80% ethanol in a beaker, covered with aluminum foil, and allowed to steep at ambient temperature for 72 hours. Following the extraction, the mixture was filtered, and the resulting filtrate was concentrated through evaporation at 60 °C for 45–60 minutes.

The characterization of the bioactive compounds was conducted utilizing high-performance liquid chromatography. An HPLC system featuring a reversed-phase C18 column was utilized. The mobile phase was composed of a 50:50 mixture of acetonitrile and purified water. Before application, all solvents were filtered using a hydrophilic polypropylene membrane with a 0.2 μm pore size and subsequently degassed via ultrasonication. The chromatographic analysis was conducted using a flow rate of 1 mL/min, an injection volume of 20 0L, and a total run time of 15 minutes for each sample. The column was operated at a constant temperature of 25 0C, with detection achieved via UV absorbance at 283 nm.

Fabrication of film

The film will be produced by Gao *et al*, (2022), with some modifications. The control film was prepared using a solution casting method. 2 g of κ-carrageenan mixed with 150 mL of distilled water was put into a beaker filled with magnetic stirrers at a temperature of 90 ℃. Then, 3% of curcumin is added to the solution. Films of CLC 0.15%, CLC 0.30%, and CLC 0.45% are provided with the same formulation and added with limonene at different concentrations of 0.15% (v/v), 0.30% (v/v), and 0.45% (v/v), respectively. The solution is then stirred for 30 minutes, poured into the Petri plate, and allowed to dry for 48 hours at room temperature.

Moisture content

The prepared films were dried at 105 °C for 24 h. The wet weight (W_{wet}) and dry weight (W_{dry}) were recorded by measuring the films before and after the drying process. Moisture content was then calculated using the following formula, as described by AOAC (1990):

$$\text{Moisture content (\%)} = \left[\frac{(W_{wet} - W_{dry})}{W_{dry}}\right] x\ 100\ \%$$

Water solubility

The initial dry weight of each film sample ($W_{initial}$) was recorded after drying at 105 °C for 24 h. The films were then immersed in distilled water for 24 h, after which they were removed and dried again at 105 °C for an additional 24 h. The final dry weight (W_{final}) was subsequently measured. Film solubility was calculated using the following equation, as described by Bhattarai and Janaswamy (2023):

$$\text{Water solubility (\%)} = \left[\frac{(W_{initial} - W_{final})}{W_{initial}}\right] x \ 100\%$$

Water Vapor Permeability (WVP)

The water vapor permeability (WVP) of the films was determined using the ASTM E96 "cup method," a standard gravimetric test for measuring water vapor transmission (ASTM E96). Plastic cups with a diameter of approximately 9 cm were filled with 50 g of silica gel. The films were secured over the mouth of each cup using cellophane tape and aluminium foil to ensure an airtight seal. The cups were then placed in a desiccator containing distilled water and maintained at 20 °C. The weight of each cup was recorded every 24 h for 5 consecutive days. The weight change over time was plotted, and linear regression analysis was performed ($r^2 > 0.99$). The water vapor transmission rate (WVTR) was calculated as the slope of weight change (g/s) divided by the test area (m²). Finally, WVP was determined based on a combination of Fick's and Henry's laws of gaseous diffusion through films, using the following equation (Sree and Nagaraaj, 2022):

$$\text{WVTR (g/s)/(m}^2\text{)} = \frac{slope \ (x)}{A}$$

$$\text{WVP} = \text{WVTR} \ x \ \frac{x}{\Delta P}$$

Where, A (m²) represents the film area, x (m) denotes the film thickness, and ΔP (Pa) corresponds to the difference in water vapor pressure across the film. A driving force of 2339 Pa was applied as the differential vapor pressure of water.

Film thickness

The developed biodegradable film thickness is obtained using a handheld micrometer (Wilkens-Anderson Co.) with an accuracy of 0.001 mm. The analysis is made at least five random dots on each film (da Costa *et al*., 2023).

Color analysis

Color analysis of film samples will be measured using ColorFlex Colorimeter (HunterLab, US). Film solutions are prepared and in containers prepared for this analysis. L* (darkness), a* (red-green), and b* (yellow-blue) will be measured. The total color difference (ΔE) will be calculated using the following equation (Alipour *et al.,* 2023):

$$\Delta E = \sqrt{[(L^* - L)^2 + (a^* - a)^2 + (b^* - b)^2]}$$

Opacity

A method prepared by Zhao *et al.* (2022), has been used to evaluate the opacity of the films. The UV Visible Spectrophotometer (UV-Vis) is used to analyze film absorption at 600 nm. A film is cut (3 cm x 1 cm) and placed in a cuvette. Measurements are taken triplicate while the opacity of the film is estimated to use the equation below:

$$Opacity \ (Amm^{-1}) = \frac{A_{600}}{x}$$

Where A_{600} is absorption at 600 nm, and x is the thickness of the film (mm).

Fourier-Transform Infrared Spectroscopy (FTIR)

The molecular arrangement of the films and the interactions between polymeric components were examined using Fourier-transform infrared (FTIR) spectroscopy. An Agilent Technologies Cary 630 FTIR spectrometer was employed over a spectral range of 4000–600 cm⁻¹. Spectra were acquired using the attenuated total reflectance (ATR) technique with a resolution of 4 cm⁻¹ (Maroufi *et al.,* 2021).

Field Emission Scanning Electron Microscopy (FESEM)

As for FESEM, film samples were analyzed using FESEM (JSM-7900F Schottky) with an enlargement of ×1, 500 and ×10, 000 for cross-section and surface of the films, respectively. The film sample is coated with palladium platinum for FESEM to enable and improve sample imaging (Vonnie *et al*., 2023).

Antimicrobial analysis

The antimicrobial activity of the films was evaluated using the agar diffusion method (de Oliveira *et al.,* 2020). The antimicrobial efficacy of the developed films was assessed using the agar diffusion method. *Escherichia coli* cultures were prepared in Mueller-Hinton broth and incubated at 37 °C for 18–24 hours in a shaker incubator. Isolated colonies were obtained by streaking a loopful of the bacterial stock onto Mueller-Hinton agar plates and incubating them at 37 °C for 18–24 hours. A bacterial suspension was standardized to a 0.5 McFarland turbidity using 0.85% normal saline and then inoculated onto MH

agar plates using a sterile swab. Circular film discs were subsequently placed on the surface of the inoculated agar. Streptomycin was utilized as the positive control antibiotic for the tested bacterial strains. Following incubation at 37 °C for 18–24 hours, the presence of inhibition zones around the film discs was observed.

Antioxidant analysis

The antioxidant capacity of the environmentally friendly films was determined via the 2,2-diphenyl-1-picrylhydrazyl radical scavenging assay. The procedure was adapted from Lyn *et al.* (2021) with minor modifications. To evaluate the antioxidant capacity of the eco-friendly films, a 2,2-diphenyl-1-picrylhydrazyl radical scavenging assay was performed, following a modified protocol adapted from Lyn *et al.* A 0.1 mM solution of DPPH was prepared by dissolving 4 mg of DPPH in 100 mL of methanol. Subsequently, 20 mg of each film sample was introduced into 4 mL of the freshly prepared DPPH solution. The resulting mixtures were incubated in darkness at ambient temperature for 30 minutes. The absorbance of these solutions was then measured at 517 nm using a UV-Vis spectrophotometer. The percentage of DPPH radical scavenging activity for the biodegradable films was subsequently determined using the following equation:

$$\text{DPPH scavenging effect (\%)} = \left[\frac{(A_{DPPH} - A_{extract})}{A_{DPPH}}\right] \times 100\%$$

A_{DPPH} and $A_{extract}$ are the absorption values of DPPH ethanol solutions and sample extracts respectively at 517 nm. Pure ethanolic solution without DPPH is used as a correlate. Each sample is tested in triplicates.

Storage stability

The storage stability of the CLC films was evaluated over 14 days using the gravimetric method described by Erna *et al.* (2022). Films containing varying concentrations of limonene extract (0.15%, 0.30%, and 0.45%) were stored under three conditions: room temperature (25 °C), incubator (37 °C), and cold storage (4 °C), each maintained at 50% relative humidity (RH). The initial mass of the films was recorded on Day 0, and subsequent measurements were taken on Days 7 and 14 to determine the final mass.

Biodegradability

The biodegradability of the composite films in soil was assessed with slight modifications to the method described by Choudhary *et al.* (2023). Soil was placed in plastic containers to a depth of approximately 4 cm. The films were cut into square specimens (2 cm × 2 cm) and buried 2 cm below the soil surface. The initial mass (M_0) of each container, including the buried films, was recorded, and the containers were maintained at ±25 °C. The containers with the degrading films and associated residues were weighed daily for 5 days. The percentage of biodegradation of the films was then calculated using the following equation:

$$Biodegradability \ (\%) = \left[\frac{(M_0 - M_{1)}}{M_0} \right] x \ 100\%$$

M_0 (g) is the initial weight of a plastic container grown with the original film before biodegradation testing, and M_1 (g) is the weight of a plastic tray buried with film residue after biodegradable testing.

pH sensitivity

Hypoxanthine (HX) solutions mixed with pH 1 to pH 14 have reacted with three solutions of the κ-carrageenan-limonene-curcumin (CLC) film with varying concentrations: 0.15% CLC film, 0.30% CLC film and 0.45%. Color changes of each solution of the CLC film have been observed and measured using a UV-Vis spectrophotometer. 0.01 M HX was prepared and placed in a centrifugal tube. Each centrifugal tube contains 10 mL 0.01 M HX, whose pH ranges from 1 to 14. Different pH levels of 0.01 M HX have responded to CLC film and further analyzed using UV–Vis (Xiang *et al.*, 2023).

Real sample analysis

Using biodegradable films with an indicator of freshness in observing chicken breast damage will be carried out following Said and Sarbon, (2023), with slight modifications. First, 10 g of raw chicken meat is cut into squares (4 cm x 4 cm). Then, fresh chicken meat is placed on a petri dish and closed using a cover patched with a different film of limonene concentration. All samples are stored at room temperature (25-28 °C) and noticed within five days of storage time. Film color changes are monitored and measured.

Statistical analysis

Statistical analysis was conducted using IBM SPSS Statistics, version 29. One-way analysis of variance was employed to assess differences between components and treatment levels, with Tukey's post-hoc test utilized for multiple comparisons. A significance level of $p < 0.05$ was adopted, and all experimental trials were performed in triplicate, with outcomes presented as mean ± standard deviation.

Results

Extraction of crude extract of limonene from orange peel

Limonene, the main component of orange essential oil, a citrus scent and is identified at 3.392 min using High Performance-Liquid Chromatography (HPLC). α-pinene (3.834 min), β-pinene (5.486 min), myrcene (5.866 min), limonene oxide (6.303 min), linalool (6.645 min) and α-terpineol (6.917 min) (Fan *et al.*, 2015). The appearance of the developed films is shown in Figure 1.
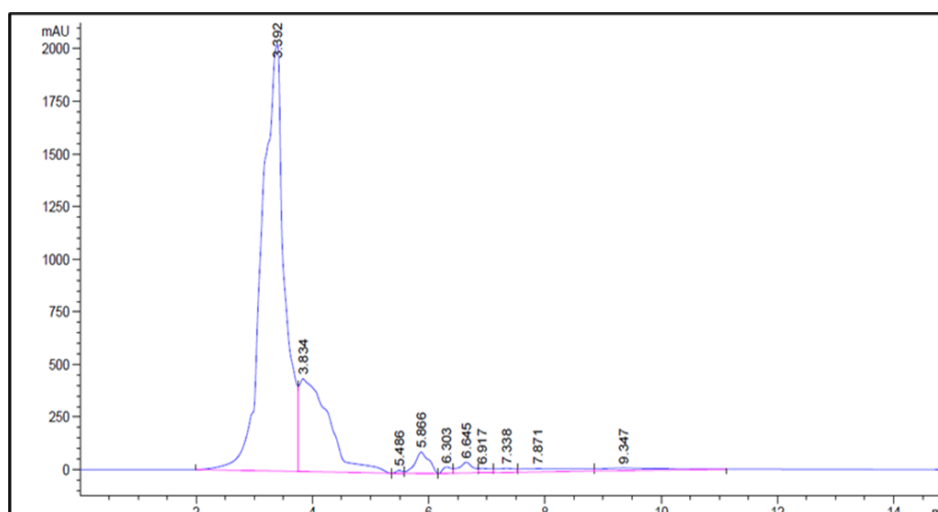

Figure 1. HPLC limonene analysis where the main peak at 3.834 minutes is limonene

Physicochemical properties

Thickness film, opacity, and water hydrophobic properties including moisture content, water solubility and water vapor permeability were used to evaluate the films comprehensively based on Table 1 and Figure 2. Control films showed higher moisture content, water solubility, water vapor permeability, film thickness, and opacity compared with CLC films.

Table 1. Moisture content (%), Film thickness (mm), Water solubility (%), Water vapor permeability $(gs^{-1} m Pa)$ (10^{-6}) dan Opacity (Amm)

Parameter	Control	CLC 0.15%	CLC 0.30%	CLC 0.45%
Moisture Content (%)	12.90 ± 3.54^a	6.68 ± 2.28^a	8.88 ± 3.60^a	7.98 ± 1.95^a
Film thickness (mm)	0.02 ± 0.01^a	0.01 ± 0.00^a	0.00 ± 0.01^a	0.01 ± 0.01^a
Water solubility (%)	12.29 ± 0.28^a	9.18 ± 0.40^b	8.64 ± 0.37^b	7.41 ± 0.09^c
Water vapor permeability $(gs^{-1} m Pa)$ (10^{-6})	33.12 ± 1.59^a	8.58 ± 0.32^b	9.62 ± 0.41^b	9.61 ± 0.30^b
Opacity	22.32 ± 8.60^a	20.68 ± 5.32^a	17.31 ± 2.73^a	20.47 ± 4.14^a

The value represents an average of ± standard deviations of the three replications. Different letters (in rows) show significant differences (one-way ANOVA, Tukey's HSD test, $p < 0.05$.
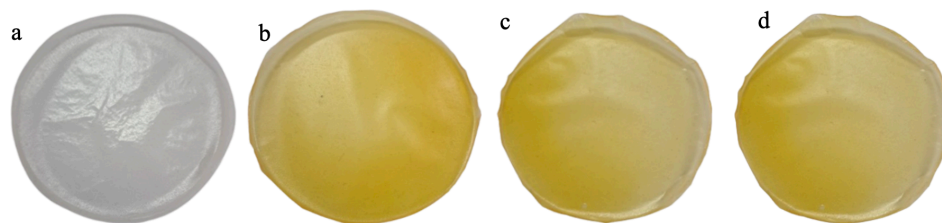

Figure 2. The appearance of the (a) control film, (b) CLC 0.15% film, (c) CLC 0.30% film, and (d) CLC 0.45% film

Changes in the colour of the film were evaluated by measuring L* (light/dark), a* (red/green) and b* (yellow/blue) according to Table 2. The control films' L*, a*, and b* values were significantly higher than those of CLC 0.15%, CLC 0.30%, and CLC 0.45%. The a* values of the film exhibited a shift from negative to positive, suggesting a change from green to red colour of the

1762

films. The b* values of the film exhibited a shift from negative to positive, suggesting a change from blue to yellow colour of the films. There were no significant differences between CLC films and control film.

Table 2. L, a, b, and ΔE for control film, CLC 0.15%, CLC 0.30%, and CLC 0.45%

Film	L	a	b	ΔE
Control	12.61 ± 0.06^d	-0.67 ± 0.20^d	-1.76 ± 0.33^d	82.14 ± 0.06^a
CLC 0.15%	43.33 ± 0.63^c	2.84 ± 0.35^a	57.47 ± 0.95^c	74.71 ± 0.28^d
CLC 0.30%	50.43 ± 0.01^a	1.05 ± 0.04^c	68.74 ± 0.14^a	79.01 ± 0.12^b
CLC 0.45%	47.15 ± 0.16^b	1.73 ± 0.05^b	63.79 ± 0.13^b	76.95 ± 0.17^c

The value represents an average of ± standard deviations of the three replications. Different letters (in columns) show significant differences (one-way ANOVA, Tukey's HSD test, $p < 0.05$).

The films' surface and cross-section were analysed using Field Emission Scanning Electron Microscopy (FESEM) as shown in Figure 3. Control film showed a homogeneous and compact structure without air bubbles, pores, cracks, or droplets. However, the increases of limonene concentration made the surface of the films smoother and the increased of small particles of limonene on the surface of k-carrageenan-based film. From the films' cross section, the film structure's uniformity increased as the limonene concentration increased.

A close range of this film's chemical composition and bonding patterns is shown in Figure 4. There were seven observed characteristic peaks: O-H, C-H, C=C, C-O, C-OH, sulphate ester groups O=S=O, C=O=C stretch and $CO-O-SO_3$ stretch.
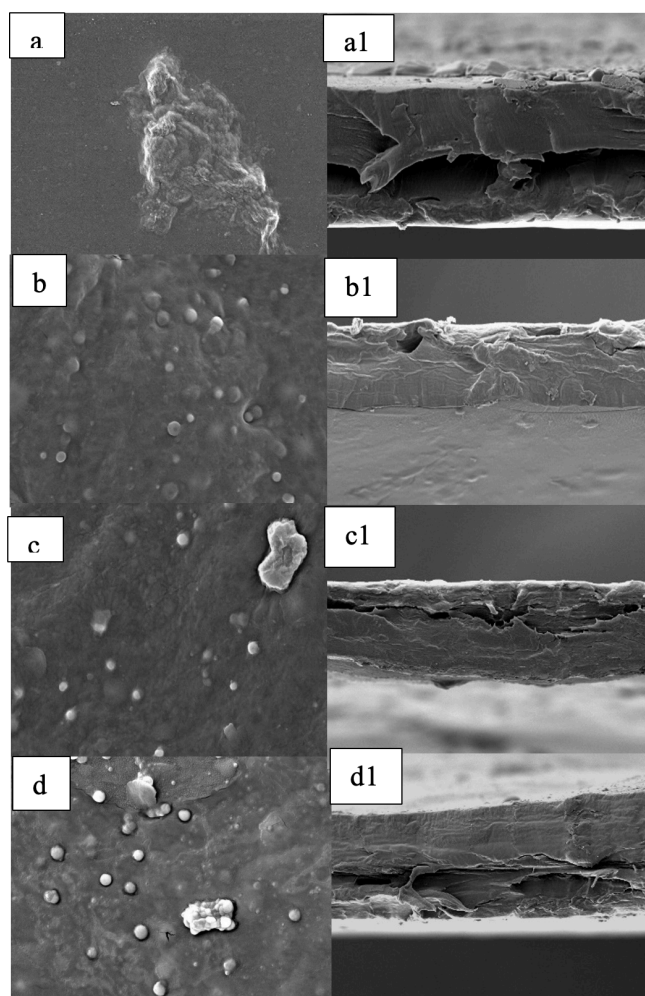
Figure 3. Images of FESEM (a) control, (b) CLC 0.15%, (c) CLC 0.30% and (d) CLC 0.45% film at an enlargement of ×10,000 with cross-sectional images (a1) control, (b1) CLC 0.15%, (c1) CLC 0.30%, and (d1) CLC 0.45% film at ×1500 magnification
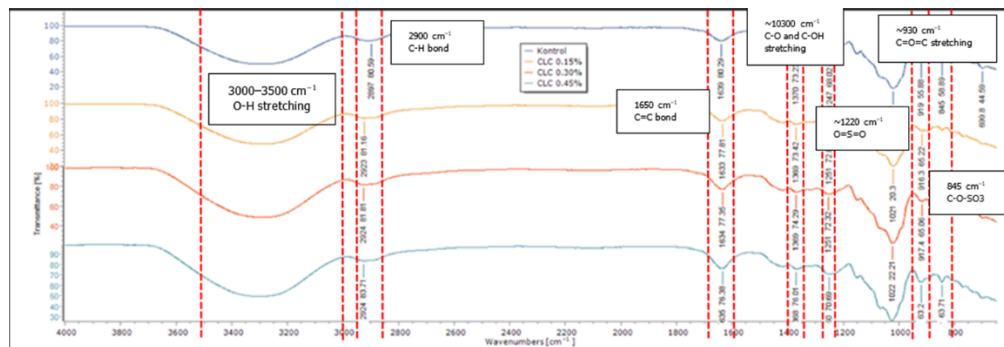
Figure 4. Spectrum FTIR (a) control, (b) CLC 0.15%, (c) CLC 0.30%, and (d) CLC 0.45% film

The efficiency of the film

The inhibition zone for the film of CLC 0.30% was higher than CLC film 0.15% (Table 3). However, no inhibition zone is observed for control and CLC 0.45% film. The results showed that the antioxidants property of the film increased as the concentration of limonene increased which compared to the control film.

Table 3. Inhibition zones for antimicrobial and antioxidant activity of the control film, CLC 0.15%, CLC 0.30% and CLC 0.45%

Film	Inhibition zone (cm^2)	DPPH$_{scavenge}$ (%)
	Escherichia coli	
Control	0.00 ± 0.00^c	-66.49 ± 42.87^b
CLC 0.15%	2.21 ± 0.01^b	-1.96 ± 1.58^a
CLC 0.30%	2.42 ± 0.01^a	8.03 ± 2.80^a
CLC 0.45%	0.00 ± 0.00^c	13.17 ± 0.48^a

The value represents an average of ± standard deviations of the three replications. Different letters (in rows) show significant differences (one-way ANOVA, Tukey's HSD test, $p < 0.05$).

Storage stability of the films was observed in three different conditions: room temperature, incubator, and chiller. Among three different conditions, the films were more stably kept in a cold room. The films were observed a decreasing mass at day 7 and decreasing at day 14 except for those stored in room temperature at shown in Figure 5.
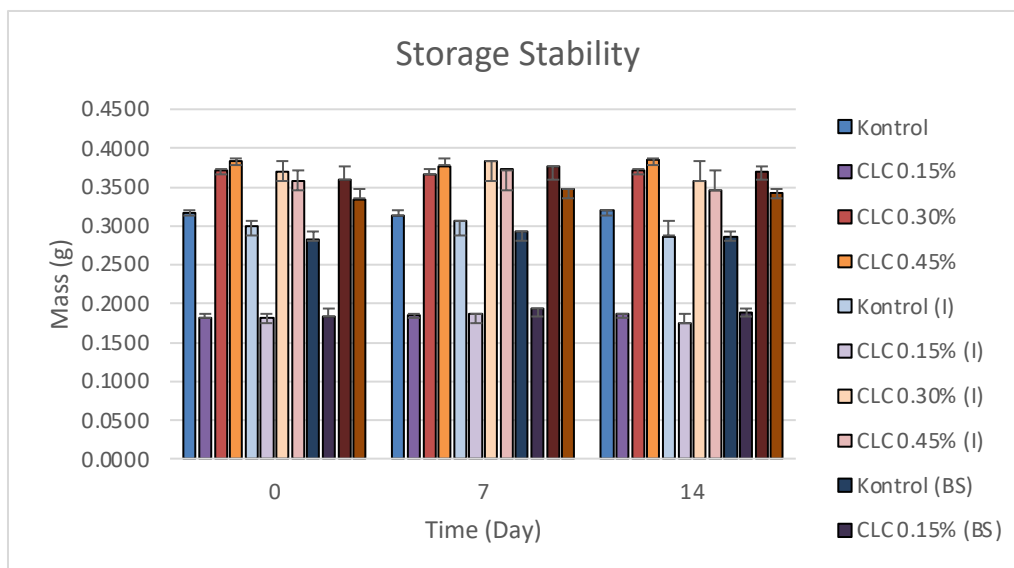
Figure 5. Control Film Storage Stability, CLC 0.15%, CLC 0.30% and CLC 0.45% on three conditions: room temperature, incubator (I) and Chiller (BS)

The biodegradability of CLC films decreased with increased limonene concentration as compared with control films. CLC 0.30% showed the highest biodegradability percentage compared with other film.

Table 4. Biodegradability (%) of control film, CLC 0.15% film, CLC 0.30% film, and CLC 0.45% film

Films	Biodegradability (%)
Control	14.80 ± 4.84^b
CLC 0.15%	37.76 ± 15.15^{ab}
CLC 0.30%	60.01 ± 13.59^a
CLC 0.45%	35.78 ± 3.13^{ab}

The value represents an average of ± standard deviations of the three replications. Different letters (in columns) show significant differences (one-way ANOVA, Tukey's HSD test, $p < 0.05$).

There was not significantly discolored from pH 2 to 9 is shown in Figure 6. The color changed from bright yellow to brown at pH 10. Only changed to reddish brown at pH 11, and only reached the wine red when exposed to pH levels of 12 and above.

Table 5. Real sample analysis of CLC 0.15% film, CLC 0.30% film, and CLC 0.45% film
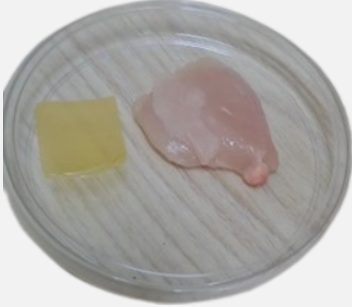
Film	Before	After
CLC 0.15%		
CLC 0.30%		
CLC 0.45%		

Figure 6. Color change of freshness indicator film for 24 hours at room temperature from pH 1 (right) to pH 13 (left)

CLC films changed the color from yellow to orange after being left for 24 hours at room temperature (Table 5). The changes of colour indicated that the chicken meat is not fresh.

Discussion

According to Cataldo *et al.* (2004), limonene can be detected by using HPLC at 3.7 minutes. There is a slight difference in retention time compared with the literature due to factors such as the method and solvent used to extract limonene. Next, the thickness of the film is decreased with the addition of limonene because limonene acts as a plasticizer in the film matrix, thus increasing the free volume of the film, increasing flexibility, and reducing the elastic modulus of the film (Roy and Rhim, 2020). The water barrier properties of the films had been improved due to the characteristics of limonene and curcumin, which are hydrophobic compounds. The film's ability to absorb moisture has been reduced (Cheng *et al.*, 2022). Limonene and curcumin also contribute to the interference of hydrogen bonding and electrostatic interactions between the polymer chains of k-carrageenan that provide stability to the hydrogel network (Yu *et al.*, 2019). Moreover, the hydrophilic region of the k-carrageenan chain interacts with limonene, thus reducing the number of binding sites available to water molecules (Fani *et al.*, 2022). The opacity of the control film was low compared to CLC films because the addition of curcumin caused a colour change, which can contribute to the opacity increase (Liu *et al.*, 2018). The curcumin added to the k-carrageenan film has the lowest size of the free-volume hole, which can affect the emission rate of curcumin (Rhim *et al.*, 2021).

The difference in colours in control film is the lowest because limonene incorporation has been linked to high glistering, which can be used for packaging applications (de Castro *et al.*, 2023). In addition, a value of "b" indicates that the yellow colour intensity of limonene and curcumin films increases compared to k-carrageenan-based control films. The surface morphology measured by FESEM showed no visible cracks, suggesting greater flexibility and strength (Arrieta *et al*., 2013). FTIR further analysed the film composition, which revealed that hydroxyl (O-H) forms hydrogen bonds that contribute to chemical reactions. The C-H bond discusses the enthalpy of thermal decomposition and the energy required to break the carrageenan bond (Ramli *et al.*, 2023).

Based on the antioxidant results, it proved that limonene has antioxidant properties naturally (de Ávila Gonçalves *et al.*, 2023) and has antimicrobial properties by causing bacterial cell changes and protein structure, leading to cell death (Lan *et al.*, 2019). The films have the stability to be stored at a cold temperature, which slows down the loss of biologically active limonene. Limonene can be degraded in two stages, one involves the thermal degradation of limonene into other aromatic compounds via a secondary conversion mechanism (Ma *et al.*, 2020). Stage two involves the formation of oxidation products that can further degrade limonene and lead to the formation of foreign flavours and odours (Li and Lu, 2016). The mechanism of action is C=C fragmentation in the limonene molecule, which may cause the formation of free radicals that will react with oxygen and form peroxide, which can further degrade limonene (Januszewicz *et al*., 2020). However, limonene and curcumin combined with k-carrageenan-based films slow the film degradation process based on the biodegradability results due to the strong interaction between limonene, curcumin, and k-carrageenan molecules. The movement of water molecules between film and soil is slowing down and exhibits high activity against microbes during the soil degradation process (Dey *et al*., 2021). pH sensitivity proved that curcumin decomposition is pH-dependent and undergoes rapid degradation at higher pH values (Lee *et al.*, 2013). Priyadarsini (2014) reports that completely deprotonated curcumin appears red at pH 10 and above, where the absorption maximum is 467 nm. Furthermore, the degradation reaction of curcumin continues rapidly at higher pH levels compared to lower pH levels (Schneider *et al.*, 2015). The colour changes in the real sample analysis showed a reaction between curcumin and hypoxanthine. The mechanism is that curcumin reacts with hypoxanthine, where hypoxanthine has purine-containing nitrogen (Brychkova *et al.*, 2008). The protonation of nitrogen increases, leading to darker colour changes.

In conclusion, the physicochemical properties of the film can be characterized. The stability of the k-carrageenan-based film have been improved

with the addition of limonene and curcumin especially the water barrier properties. The moisture content, water solubility, and water vapor permeability have been improved as the addition of limonene in the k-carrageenan-based film have reduced the number of binding sites of the water molecules. The films' antioxidant and antimicrobial properties also proved that naturally limonene have the antimicrobial and antioxidant functional properties. The colour changes of the CLC films proved the capability of the films as the freshness indicator due to the reaction between curcumin and nitrogen compound. However, the range of colour changes can be improved by combining the curcumin with other natural dye such as anthocyanin. On the other hand, the variety of the sample also can be enhanced by using other samples such as fish, prawn, and meat.

Acknowledgements

Conflicts of interest

The authors declare that there are no conflicts of interest regarding the publication of this paper.

References

Abedi-Firoozjah, R., Salim, S. A., Hasanvand, S., Assadpour, E., Azizi-Lalabadi, M., Prieto, M. A. and Jafari, S. M. (2023). Application of smart packaging for seafood: A comprehensive review. Comprehensive reviews in food science and food safety, 22:1438-1461.

Alipour, A., Rahaiee, S., Litkohi, H. R., Jamali, S. N. and Jafari, S. M. (2023). Development and optimization of whey protein-Lepidium perfoliatum gum packaging films: An approach towards antimicrobial and biodegradable films. Industrial Crops and Products, 196:116447.

AOAC. (1990). Official methods of analysis of the AOAC, 15th ed. Methods 932.06,925.09, 985.29, 923.03. Association of official analytical chemists. Arlington, VA, USA.

Arrieta, M. P., López, J., Ferrándiz, S. and Peltzer, M. A. (2013). Characterization of PLA limonene blends for food packaging applications. Polymer Testing, 32:760,768.

Barbosa, M. H. R., Goncalves, S. D. A., Marangoni Junior, L., Alves, R. M. V. and Vieira, R. P. (2022). Physicochemical properties of chitosan-based films incorporated with limonene. Journal of Food Measurement and Characterization, 16:2011-2023.

Bhattarai, S. and Janaswamy, S. (2023). Biodegradable films from the lignocellulosic residue of switchgrass. Resources, Conservation and Recycling, 201:107322.

Brychkova, G., Fluhr, R. and Sagi, M. (2008). Formation of xanthine and the use of purine metabolites as a nitrogen source in Arabidopsis plants. Plant Signaling & Behavior, 3:999-1001.

Cataldo, F., Keheyan, Y. and Baccaro, S. (2004). Gamma-radiolysis of chiral molecules: R (+)-limonene, S (-)-limonene and R (-)-a-phellandrene. Journal of radioanalytical and nuclear chemistry, 262:423-428.

Cheng, C., Chen, S., Su, J., Zhu, M., Zhou, M., Chen, T. and Han, Y. (2022). Recent advances in carrageenan-based films for food packaging applications. Frontiers in Nutrition, 9:1004588.

Choudhary, S., Sharma, K., Mishra, P. K., Kumar, V. and Sharma, V. (2023). Development and characterization of biodegradable agarose/gumneem/nanohydroxyapatite/polyoxyethylene sorbitan monooleate based edible bio-film for applications towards a circular economy. Environmental Technology & Innovation, 29:103023.

da Costa, R. D. S., Flôres, S. H., Brandelli, A., Vargas, C. G., Ritter, A. C., da Cruz Rodrigues, A. M. and da Silva, L. H. M. (2023). Development and properties of biodegradable film from peach palm (Bactris gasipaes). Food Research International, 173:113172.

de Ávila Gonçalves, S., Barbosa, M. H. R., Júnior, L. M., Alves, R. M. V. and Vieira, R. P. (2023). Poly (limonene): A novel renewable oligomeric antioxidant and UV-light blocking additive for chitosan-based films. Food Packaging and Shelf Life, 37:101085.

de Castro, L. L., Silva, L. G., Abreu, I. R., Cristiano, J. F., Rodrigues, S. C., Moreira Araújo, R. S. D. R., Folkersma, R., de Carvalho, L. H., Barbosa, R. and Alves, T. S. (2023). Biodegradable PBAT/PLA blend films incorporated with turmeric and cinnamomum powder: A potential alternative for active food packaging. Food Chemistry, 138146.

de Oliveira, T. V., de Freitas, P. A. V., Pola, C. C., da Silva, J. O. R., Diaz, L. D. A., Ferreira, S. O. and de FF Soares, N. (2020). Development and optimization of antimicrobial active films produced with a reinforced and compatibilized biodegradable polymers. Food Packaging and Shelf Life, 24:100459.

Determination of D-limonene content of volatile oil clathrates by HPLC. (2023). Academic Journal of Materials & Chemistry, 4:https://doi.org/10.25236/ajmc.2023.040202

Dey, D., Dharini, V., Selvam, S. P., Sadiku, E. R., Kumar, M. M., Jayaramudu, J. and Gupta, U. N. (2021). Physical, antifungal, and biodegradable properties of cellulose nanocrystals and chitosan nanoparticles for food packaging application. Materials Today: Proceedings, 38:860-869.

Erna, K. H., Felicia, W. X. L., Rovina, K., Vonnie, J. M. and Huda, N. (2022). Development of curcumin/rice starch films for sensitive detection of hypoxanthine in chicken and fish meat. Carbohydrate Polymer Technologies and Applications, 3:100189.

Fani, N., Enayati, M. H., Rostamabadi, H. and Falsafi, S. R. (2022). Encapsulation of bioactives within electrosprayed κ-carrageenan nanoparticles. Carbohydrate Polymers, 294:119761.

Gao, L., Liu, P., Liu, L., Li, S., Zhao, Y., Xie, J. and Xu, H. (2022). κ-carrageenan-based pH-sensing films incorporated with anthocyanins or/and betacyanins extracted from purple sweet potatoes and peels of dragon fruits. Process Biochemistry, 121:463-480.

Hasibuan, R. and Gultom, E. (2021). The effect of method, type of solvent and extraction time towards the yield of oil on essential oil extraction from lime peel (*Citrus aurantifolia*). In : IOP Conference Series: Materials Science and Engineering, IOP Publishing, 1122:012108.

Januszewicz, K., Kazimierski, P., Kosakowski, W. and Lewandowski, W. M. (2020). Waste tyres pyrolysis for obtaining limonene. Materials, 13:1359.

Lan, W., Liang, X., Lan, W., Ahmed, S., Liu, Y. and Qin, W. (2019). Electrospun Polyvinyl Alcohol/d-Limonene Fibers Prepared by Ultrasonic Processing for Antibacterial Active Packaging Material. Molecules (Basel, Switzerland), 24:767.

Lee, W. H., Loo, C. Y., Bebawy, M., Luk, F., Mason, R. S. and Rohanizadeh, R. (2013). Curcumin and its derivatives: their application in neuropharmacology and neuroscience in the 21st century. Current neuropharmacology, 11:338-378.

Li, P. H. and Lu, W. C. (2016). Effects of storage conditions on the physical stability of D-limonene nanoemulsion. Food Hydrocolloids, 53:218-224.

Liu, J., Wang, H., Wang, P., Guo, M., Jiang, S., Li, X. and Jiang, S. (2018). Films based on κ-carrageenan incorporated with curcumin for freshness monitoring. Food Hydrocolloids, 83:134-142.

Liu, Y., Liu, M., Zhang, L., Cao, W., Wang, H., Chen, G. and Wang, S. (2022). Preparation and properties of biodegradable films made of cationic potato-peel starch and loaded with curcumin. Food Hydrocolloids, 130:107690.

Liu, Y., Zhang, X., Li, C., Qin, Y., Xiao, L. and Liu, J. (2020). Comparison of the structural, physical and functional properties of κ-carrageenan films incorporated with pomegranate flesh and peelextracts. International journal of biological macromolecules, 147:1076-1088.

Lyn, F. H., Tan, C. P., Zawawi, R. M. and Hanani, Z. N. (2021). Physicochemical properties of chitosan/graphene oxide composite films and their effects on storage stability of palm-oil based margarine. Food Hydrocolloids, 117:106707.

Ma, S., Leong, H., He, L., Xiong, Z., Han, H., Jiang, L., Wang, Y., Hu, S., Su, S. and Xiang, J. (2020). Effects of pressure and residence time on limonene production in waste tires pyrolysis process. Journal of Analytical and Applied Pyrolysis, 151:104899.

Maroufi, L. Y., Ghorbani, M., Tabibiazar, M., Mohammadi, M. and Pezeshki, A. (2021). Advanced properties of gelatin film by incorporating modified kappa-carrageenan and

zein nanoparticles for active food packaging. International Journal of Biological Macromolecules, 183:753-759.

Priyadarsini K. I. (2014). The chemistry of curcumin: from extraction to therapeutic agent. Molecules (Basel, Switzerland), 19:20091-20112.

Rachtanapun, P., Klunklin, W., Jantrawut, P., Jantanasakulwong, K., Phimolsiripol, Y., Seesuriyachan, P., Leksawasdi, N., Chaiyaso, T., Ruksiriwanich, W., Phongthai, S. and Sommano, S. R. (2021). Characterization of chitosan film incorporated with curcumin extract. Polymers, 13:963.

Ramli, N. A., Adam, F., Mohd Amin, K. N., Nor, A. M. and Ries, M. E. (2023). Evaluation of mechanical and thermal properties of carrageenan/hydroxypropyl methyl cellulose hard capsule. The Canadian Journal of Chemical Engineering, 101:1219-1234.

Rhim, J. W., Kuzeci, S., Roy, S., Akti, N., Tav, C. and Yahsi, U. (2021). Effect of free volume on curcumin release from various polymer-based composite films analyzed using positron annihilation lifetime spectroscopy. Materials, 14:5679.

Roy, S., & Rhim, J. W. (2020). Carboxymethyl cellulose-based antioxidant and antimicrobial active packaging film incorporated with curcumin and zinc oxide. *International journal of biological macromolecules*, *148*, 666-676.

Said, N. S. and Sarbon, N. M. (2023). Monitoring the freshness of fish fillets by colorimetric gelatin composite film incorporated with curcumin extract. Biocatalysis and Agricultural Biotechnology, 50:102722.

Schneider, C., Gordon, O. N., Edwards, R. L. and Luis, P. B. (2015). Degradation of Curcumin: From Mechanism to Biological Implications. Journal of agricultural and food chemistry, 63:7606-7614.

Shaikh, S., Yaqoob, M. and Aggarwal, P. (2021). An overview of biodegradable packaging in food industry. Current Research in Food Science, 4:503-520.

Shaw, D., Tripathi, A. D., Paul, V., Agarwal, A., Mishra, P. K. and Kumar, M. (2023). Valorization of essential oils from citrus peel powder using hydro-distillation. Sustainable Chemistry and Pharmacy, 32:101036.

Sree, G. V. and Nagaraaj, P. (2022). Enhancement of PVA packaging properties using calcined eggshell waste as filler and nanonutrient. Materials Chemistry and Physics, 291:126611.

Subbuvel, M. and Kavan, P. (2022). Preparation and characterization of polylactic acid/fenugreek essential oil/curcumin composite films for food packaging applications. International Journal of Biological Macromolecules, 194:470-483.

Varadaiah, Y. G. C., Sivanesan, S., Nayak, S. B. and Thirumalarao, K. R. (2022). Purine metabolites can indicate diabetes progression. Archives of Physiology and Biochemistry, 128:87-91.

Vonnie, J. M., Rovina, K., 'Aqilah, N. M. N. and Felicia, X. W. L. (2023). Development and Characterization of Biosorbent Film from Eggshell/Orange Waste Enriched with Banana Starch. Polymers, 15:2414.

Xiang, H., Chen, X., Gao, X., Li, S., Zhu, Z., Guo, Z. and Cheng, S. (2023). Fabrication of ammonia and acetic acid-responsive intelligent films based on grape skin anthocyanin via adjusting the pH of film-forming solution. International Journal of Biological Macromolecules,128787.

Yildiz, E. (2022). Utilization Of Curcumin and Biodegradable Polymers In Intelligent And Active Food Packaging.

Yu, H. C., Li, C. Y., Du, M., Song, Y., Wu, Z. L. and Zheng, Q. (2019). Improved toughness and stability of κ-carrageenan/polyacrylamide double-network hydrogels by dual cross-linking of the first network. Macromolecules, 52:629-638.

Zhao, J., Wang, Y. and Liu, C. (2022). Film transparency and opacity measurements. Food Analytical Methods, 15:2840-2846.